Identification of new states in ^{26}Si using the ^{29}Si(^{3}He,^{6}He)^{26}Si reaction and consequences for the ^{25}Al$(p,\gamma)^{26}$Si reaction rate in explosive hydrogen burning environments

J. A. Caggiano, W. Bradfield-Smith,* R. Lewis, P. D. Parker, and D. W. Visser
Wright Nuclear Structure Laboratory, Yale University, New Haven, Connecticut 06520

J. P. Greene and K. E. Rehm
Physics Division, Argonne National Laboratory, Argonne, Illinois 60439

D. W. Bardayan
Physics Division, Oak Ridge National Laboratory, Oak Ridge, Tennessee 37831

A. E. Champagne
Triangle Universities Nuclear Laboratory, Duke University, Durham, North Carolina 27708
(Received 29 November 2001; published 9 May 2002)

We have studied the ^{29}Si(^{3}He,^{6}He)^{26}Si reaction and have identified new states in ^{26}Si at $E_x=5.140(10)$, $E_x=5.678(8)$ MeV, and $E_x=5.945(8)$. Based on these measurements and other recent evidence, we suggest spin-parity assignments of 1^+ for the 5.678 MeV state and 3^+ for the 5.945 MeV state, which would account for all the ''missing'' unnatural parity states in ^{26}Si in the excitation energy region important to hydrogen burning in novae. New reaction rates are presented for the ^{25}Al$(p,\gamma)^{26}$Si reaction based on this possible assignment of states.

DOI: 10.1103/PhysRevC.65.055801 PACS number(s): 26.30.+k, 25.40.Lw, 25.55.Hp, 27.30.+t

I. INTRODUCTION

The rate of production of ^{26}Al in its ground state (denoted as ^{26}Al^0) is currently a key question in the field of nuclear astrophysics. ^{26}Al^0 has a half-life of 7.2×10^5 yr and its β decay is followed (99.7% of the time) by a prompt 1.809 MeV γ-ray which has been identified by orbiting γ-ray telescopes such the Compton Gamma-Ray Observatory (CGRO) [1]. Its detection, combined with astronomical data such as distances to the events and masses of the stars participating in the explosions, can provide a very valuable, measurable constraint on models used to understand the explosive hydrogen burning process in novae and supernovae.

The key nuclear physics uncertainty in the production of ^{26}Al^0 in nova sites in the galaxy is the rate of the reaction sequence

$$^{24}\mathrm{Mg}(p,\gamma)^{25}\mathrm{Al}(p,\gamma)^{26}\mathrm{Si}(\beta^+\nu)^{26m}\mathrm{Al}(\beta^+\nu)^{26}\mathrm{Mg}^0,$$

which bypasses the

$$^{25}\mathrm{Al}(\beta^+\nu)^{25}\mathrm{Mg}(p,\gamma)^{26}\mathrm{Al}^0(\beta^+\nu)^{26}\mathrm{Mg}^*(\gamma)^{26}\mathrm{Mg}^0$$

reaction sequence. It is the decay of ^{26}Al^0 via the first excited state of ^{26}Mg that produces the 1.809 MeV γ rays observed by instruments such as CGRO.

In the competition between the ^{25}Al$(\beta^+\nu)$ decay and the ^{25}Al$(p,\gamma)^{26}$Si reaction, the current uncertainty is due to the lack of nuclear structure information just above the proton threshold in ^{26}Si [$S_p=5.518(3)$ MeV]. Until recently, ^{26}Si had been studied with the ^{28}Si$(p,t)^{26}$Si [2] and ^{24}Mg(^{3}He,n)^{26}Si [3,4] reactions, which preferentially populate natural parity states. In addition, those studies were conducted with energy resolutions of 140–200 keV, so that closely spaced states may not have been resolved. Iliadis *et al.* [5] made a detailed survey of the past data on ^{26}Si and derived tentative spin assignments based on these results, in conjunction with shell model calculations and mirror nucleus considerations. They concluded that the ^{25}Al$(p,\gamma)^{26}$Si rate is probably dominated by a 3^+ state (an $l=0$ resonance) which they calculated to lie at $E_x=5970(100)$ keV in ^{26}Si. This state has never been observed experimentally, including in a recent remeasurement of the ^{28}Si$(p,t)^{26}$Si reaction [6], and hence its location, its properties, and thus the ^{25}Al$(p,\gamma)^{26}$Si reaction rate are very uncertain.

Additionally, the second strongest contributors to the ^{25}Al$(p,\gamma)^{26}$Si reaction at nova temperatures are expected to be a 0^+, 4^+ doublet at 5.940(25) keV, which has never been resolved due to insufficient resolution of past experimental studies. Angular distribution measurements of the (^{3}He,n) reaction populating a state at 5.91 MeV could only be fit with a combination of 0^+ and 4^+ states [3].

Because of these numerous uncertainties in the nuclear structure of ^{26}Si above the proton threshold, we decided to study it via the ^{29}Si(^{3}He,^{6}He)^{26}Si reaction which had never been used before. This reaction should populate both natural and unnatural parity states in ^{26}Si.

The ^{29}Si(^{3}He,^{6}He)^{26}Si reaction has another distinct advantage over ^{28}Si$(p,t)^{26}$Si or ^{24}Mg(^{3}He,n)^{26}Si measurements. Due to the extra neutron on the α nucleus ^{28}Si, the Q value of the ^{29}Si(^{3}He,^{6}He)^{26}Si reaction is much less negative ($Q_0=-17.4$ MeV) than that of the (^{3}He,^{6}He) reaction on the inevitable α nucleus target contaminants ^{12}C ($Q_0=-31.6$ MeV) and ^{16}O ($Q_0=-30.5$ MeV). This difference in Q values provides a 13 MeV window for studying the spectrum of ^{26}Si without significant contamination.

*Present address: Physics Department, Queens University, Kingston, Ontario, Canada K7L 3N6.

Compared to the two-nucleon transfer reactions, the (^{3}He,^{6}He) reaction has two minor disadvantages: low cross sections (typically 0.1–1 μb/sr/state) and possible spectrum contamination from reactions on heavier target contaminants such as ^{13}C, ^{17}O, ^{18}O, and ^{30}Si. However, with ^{3}He beams of $\geqslant$50 pnA, these cross sections will provide enough statistics in a week long measurement. The target contaminants ^{13}C (1% in natural carbon), ^{17}O (0.04% of natural oxygen), and ^{18}O (0.2%) are already only a very small fraction of the target contaminants, and their contributions to the ^{6}He spectrum can be explicitly measured with enriched targets.

II. EXPERIMENT

The ^{29}Si(^{3}He,^{6}He)^{26}Si reaction was studied at 51 MeV and at 7.5° using the Enge Split-Pole spectrometer at the Yale University Wright Nuclear Structure Laboratory. A beam of ^{3}He was produced using a duo-plasmatron source and injected into the tandem, accelerated, and delivered to the target position of the spectrograph. Beam intensities of up to 150 pnA were incident on the targets. Two targets were used to populate states in ^{26}Si: a self-supporting 0.161 mg/cm^2 metallic target (59.5% ^{29}Si, 39.1% ^{28}Si, and 1.4% ^{30}Si), and a 0.17 mg/cm^2 $^{29}SiO_2$ (95.0% ^{29}Si, 4.7% ^{28}Si, and 0.3% ^{30}Si) target on a 0.1 mg/cm^2 carbon backing. The magnetic field of the spectrograph was set to bend the (less magnetically rigid) elastically scattered ^{3}He beam off the focal plane detector. Consequently the spectra were free of contamination from elastically and inelastically scattered ^{3}He. Due to this magnetic field setting, the ^{6}He^{2+} ions from ^{12}C(^{3}He,^{6}He)^{9}C, ^{16}O(^{3}He,^{6}He)^{13}O, and ^{28}Si(^{3}He,^{6}He)^{26}Si reactions also did not enter the focal plane detector. A 0.15 mg/cm^2 ^{30}Si target on a 0.1 mg/cm^2 carbon backing was used to deduce the spectrum contamination arising from (^{3}He,^{6}He) reaction on ^{30}Si. The spectrum taken with the metal and oxide targets were compared to measure spectrum contamination resulting from (^{3}He,^{6}He) reactions ^{17}O and ^{18}O. In addition, because of the presumably large cross section for the ^{13}C(^{3}He,^{6}He)^{10}C reaction, and because ^{13}C is 1% of natural carbon, a 0.1 mg/cm^2 target of ^{13}C was used to determine this contribution explicitly.

The focal plane detection system consisted of a gas ionization drift chamber backed by a scintillator and has been described elsewhere [7]. The detector provides two position measurements in the dispersive (x or horizontal) and nondispersive (y or vertical) directions, two energy loss measurements in the gas (100 Torr of isobutane), and a residual energy measurement in the scintillator. Using these measurements, it is possible to cleanly identify and separate the ^{6}He from the other reaction products, and measure their momentum.

Figure 1 shows the ^{6}He spectra obtained at a ^{3}He energy of 51 MeV, all measured at the same spectrometer setting. Figures 1(d) and 1(e) are the spectra from the ^{29}Si(^{3}He,^{6}He)^{26}Si reaction at 51 MeV at 7.5°, during two separate runs, taken with slightly different data acquisition systems. Figures 1(a), 1(b), and 1(c) show the spectra obtained using the ^{27}Al, ^{13}C, and ^{30}Si+C targets, respectively.

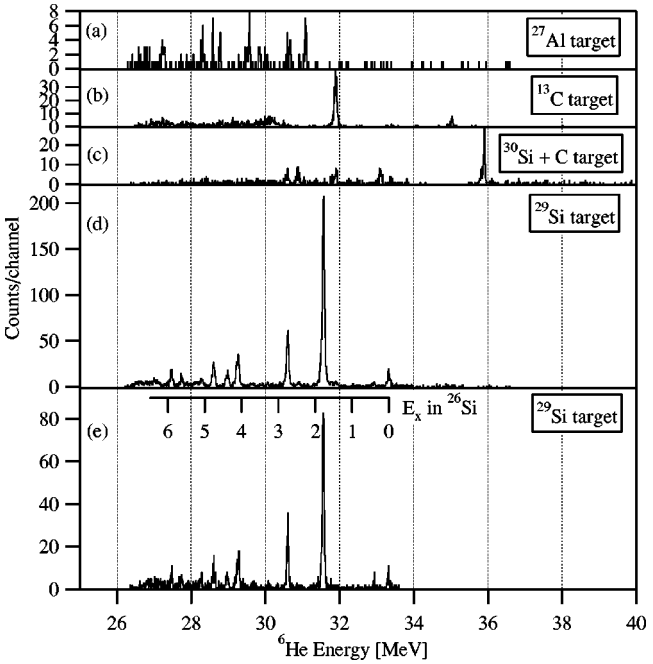

FIG. 1. ^{6}He energy spectra from the (^{3}He,^{6}He) reaction on the listed targets.

The largest contamination of the ^{26}Si spectrum originates from the ^{13}C(^{3}He,^{6}He)^{10}C(E_x=3.354 MeV) peak, which is barely visible just to the right of the largest peak in the ^{26}Si spectrum, which is the first excited state at 1.796 MeV. The transition to the ^{27}Si ground state is the largest peak in the spectrum taken with the ^{30}Si+C target, and cannot be seen in the ^{26}Si spectrum 1(d). From these background measurements, it is estimated that the spectrum in the region of interest above the proton threshold is contaminated at a level of only 1 count/channel or less, and therefore cannot possibly be the cause of the peaks shown in the two ^{26}Si spectra.

The peak just to the left of the ^{29}Si(^{3}He,^{6}He)^{26}Si(g.s.) peak in Figs. 1(d) and 1(e) is due to the high rate of α's in the detector from the dominant transition in the (^{3}He,α) reaction on the target materials. The origin of this contamination is easily identified as an α peak in Fig. 2, which shows the focal plane position versus total energy loss in the gas-filled volume [after applying a gate in the (ΔE-E) spectrum]. The peaks from the (^{3}He,^{6}He) spectrum are well localized within the gate (indicated by the outlined area in Fig. 2), whereas the α contamination peak (indicated by the arrow) appears as a vertical stripe through the spectrum. No other stripes appear anywhere else in the spectrum, ensuring that this is the only contamination peak from alpha particles detected in the focal plane detector. The ^{4}He spectrum in the region of interest, above the proton threshold in ^{26}Si, has fewer counts than this peak and far less structure. Thus, in this energy region above the proton threshold, the α contamination does not contribute significantly to the spectrum.

Figure 3 compares the spectrum taken with the silicon oxide target and the silicon metal target. This comparison determines the contamination of the spectrum due to reactions on oxygen in the targets; if the peaks in the region of interest came from the (^{3}He,^{6}He) reactions on ^{17}O and ^{18}O,

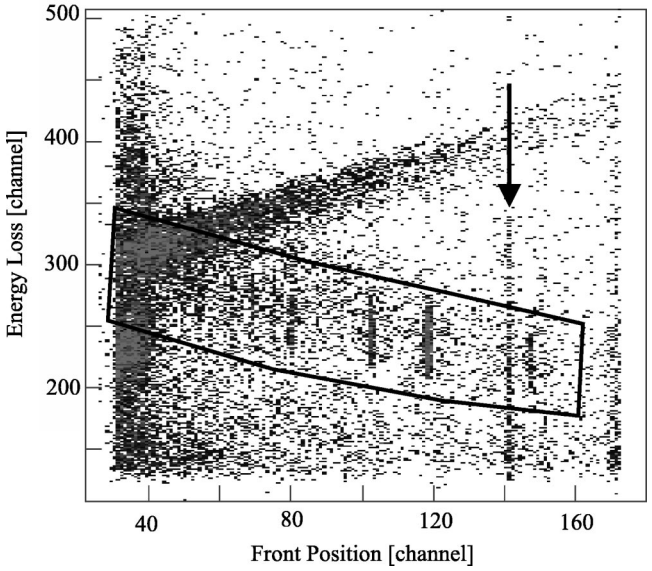

FIG. 2. Cathode (ΔE) vs front position (momentum) spectrum. The vertical stripe, indicated by the arrow, originates from pile-up due to the high rate of the (^{3}He,α) reaction. Within the outlined area (the location of the ^{6}He), this is the only ^{4}He contamination.

these peaks would be much stronger in the oxide target spectrum. The shape of the spectra are very similar for oxide and metal targets, indicating that oxygen contamination will not interfere with the spectrum interpretation.

The focal plane calibration was performed using the ^{29}Si(^{3}He,^{6}He)^{26}Si [$Q_0 = -17.413(3)$ MeV [8]] and ^{27}Al(^{3}He,^{6}He)^{24}Al [$Q_0 = -19.805(4)$ MeV [8]] reactions.

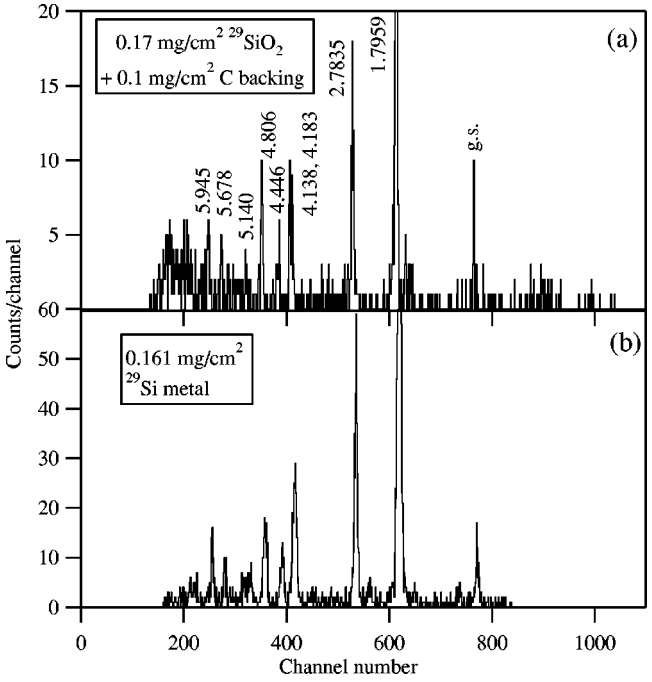

FIG. 3. Comparison between the data taken with the silicon oxide target (a) and the silicon metal target (b). Notice that the shape of the spectrum is the same, confirming that there are no peaks coming from contaminant reactions on oxygen.

The known states that were populated in these reactions were used to calibrate the magnetic rigidity as a polynomial function of the focal plane detector position [$B\rho(x)$]. This calibration function was determined using a fit extracted from the ground state and excited states in ^{24}Al at 0.4258(1), 0.510(5), 1.107(6), 1.275(9), 1.559(13), 2.349(20), 2.534(13), 2.810(20), and 3.885(25) MeV and the excited states in ^{26}Si at 1.7959(2), 2.7835(3), 4.446(3), and 4.806(2) MeV [9,10]. Fits up to third order yield the same results within a few keV, but the reduced chi-squared parameter is minimized for the linear fit. Peaks from the ^{29}Si(^{3}He,α) reaction were also used for a calibration check, to verify the linearity of the momentum dispersion at low rigidities, i.e., low focal plane detector positions. For this check, α spectra were also measured at 42 MeV, which places the known

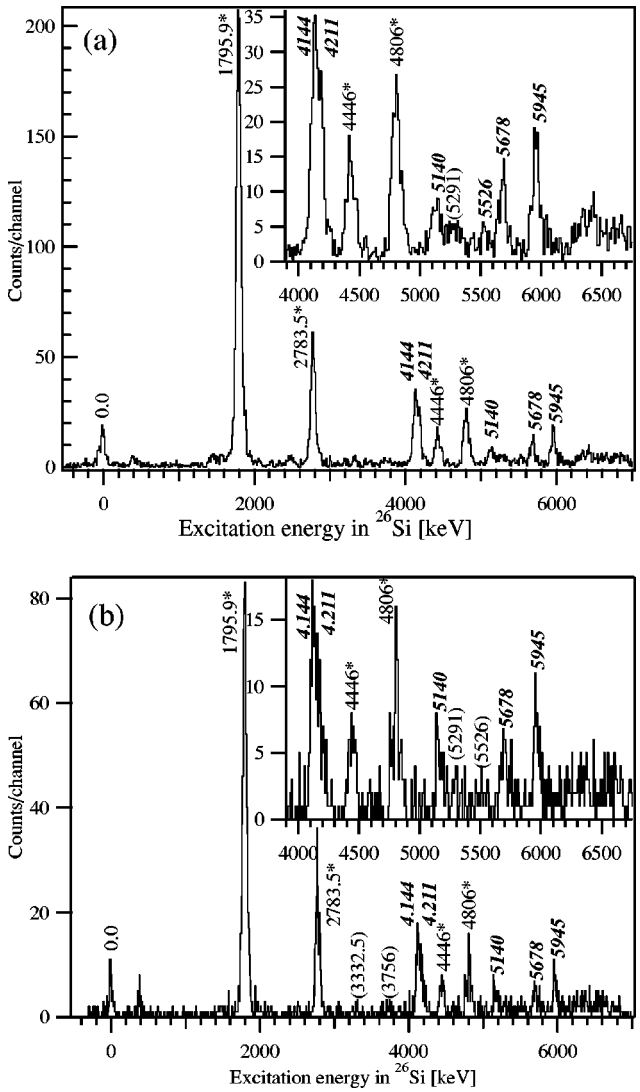

FIG. 4. Calibrated ^{26}Si excitation energy spectra from both experiments at 51 MeV and 7.5°. (a) The older, lower resolution data, and (b) the newer, higher resolution data. The states described in plain text are the previously assigned values; those marked with an asterisk were used for the focal plane calibration. The measurements presented in this work are in bold, italic text. The insets are the spectra from 3.9–6.75 MeV expanded.

TABLE I. Excitation energy measurements (in MeV) of ^{26}Si up through 6 MeV presented here, compared with the tabulated values in the literature. Our results and uncertainties are weighted averages of the two separate measurements made. Dashed lines indicate states which were not populated sufficiently for measurement. Those listed without error bars indicate that they were seen but excitation energies were not measured. Asterisks denote states which were used for calibration. All others are listed with their measured uncertainties. The last two columns are suggested values for E_x and J^π.

This work	Ref. [6]	Ref. [9]	J^π [6]	J^π [9]	J^π [5]	E_x	J^π
0.0	0.0	0.0	–	0^+	0^+	0.0	0^+
1.7959*	1.7959	1.7959(2)	–	2^+	2^+	1.7959	2^+
2.7835*	2.7835	2.7835(4)	–	2^+	2^+	2.7835	2^+
–	3.3325	3.3325(3)	–	0^+	0^+	3.3325	0^+
–	3.756	3.756(2)	–	–	3^+	3.756	3^+
–	–	3.842(2)	–	–	–		
–	–	4.093(3)	–	–	–		
4.144(8)[a]	4.155(2)	4.138(1)	2^+	2^+	2^+	4.138	2^+
4.211(16)	–	4.183(11)	–	–	4^+	4.183	3^+
4.446*	4.446	4.446(3)	$2^+ + 4^+$	–	3^+	4.446	$2^+ + 4^+$
4.806*	4.806	4.806(2)	$(0^+ + 2^+ + 4^+)$	0^+	0^+, 2^+, 4^+	4.806	$0^+ + 2^+ + 4^+$
5.140(10)	5.145(2)	–	2^+	–	–	5.145	2^+
5.291	5.291(3)	5.229(12)	4^+	–	2^+	5.291	4^+
–	–	5.330(20)	–	4^+	4^+		
5.526(8)	5.515(5)	5.562(28)	4^+	–	1^+	5.518	4^+
5.678(8)	–	–	–	–	–	5.678	1^+
–	5.916(2)	5.940(25)	0^+	0^+	0^+, 4^+	5.916	0^+
5.945(8)	–	–	–	–	–	5.945	3^+

[a]The two states at 4.144 and 4.211 are found at 4.148(5) MeV when fit as a broad single peak.

peaks in the low-bending-radius region of interest in the focal plane detector.

Figure 4 shows the calibrated excitation energy spectra from our measurements. Very small peaks appear in the spectra at the location of known states at 3.33 and 3.76, but are populated too weakly for us to draw any conclusions about them. It does not appear that we see the 4.093 MeV state listed in the literature. The previously assumed doublet at 4.138 and 4.183 MeV is populated here, but unresolved. The peak is 20% wider than adjacent peaks and is asymmetric, suggesting that it is a doublet. Fitting the peak as a doublet we measure the states at 4.144(8) and 4.211(16) MeV; fitting it as a singlet yields 4.148(8). Two previously unidentified peaks appear at 5.140(8) and 5.678(8) MeV in the ^{26}Si spectrum. A peak is visible just to the right of the 5.140 MeV peak in Fig. 4(a), which is assumed to be the 5.291 MeV state seen in Ref. [6]. We also see a state at $E_x = 5.945(8)$ MeV. Based on the weak population of the 0^+ ground state and the even weaker population of the 3.333 MeV 0^+ state, we conclude that the state we see at 5.945 MeV is not a 0^+ state. A small high energy shoulder on the peak, making it slightly wider at the base, suggests that another state lies there. However, it is too weak for us to draw any conclusions about. There is a weak state found to be at 5.526(8) MeV in our spectrum, which may be the 5.562(25) MeV state seen previously.

A summary of our measurements and a comparison with the tabulated states taken from the literature are given in Table I. The values in the table come from the weighted average of the two separate measurements, in Figs. 4(a) and 4(b). The uncertainties quoted are dominated by statistics, but include small systematic error contributions from scattering angle (0.05° which corresponds to $\leqslant 1$ keV) and calculated energy losses (5% which corresponds to $\leqslant 4$ keV). Uncertainty in the beam energy (at most 50 keV) makes only a negligible contribution (<1 keV) since the (^{3}He,^{6}He) reaction is used for the calibrations as well as the measurements. The uncertainties in the masses of ^{26}Si (3 keV) and ^{24}Al (4 keV) [8] were included in the uncertainties of the points used for calibration.

III. DISCUSSION

It is not difficult to understand why the 5.140 and 5.678 MeV states were not seen before. The ^{24}Mg(^{3}He,n)^{26}Si reaction (Ref. [4]) measurement had insufficient resolution (200 keV). However, the ^{24}Mg(^{3}He,n)^{26}Si data in Ref. [3] show a small peak in the spectrum at about 5.1 MeV, but no spin-parity assignment was made. Neither group observed the 5.678 MeV state.

The ^{28}Si(p,t)^{26}Si measurement by Paddock [2] had roughly 140 keV resolution. The 5.678 MeV state does not appear in their spectrum, and the 5.140 MeV state was obscured by a contamination from the ^{12}C(p,t)^{10}C reaction, showing the advantage of using the ^{29}Si(^{3}He,^{6}He)^{26}Si reaction.

In order to discuss the implications of these new ^{26}Si structure measurements, we have combined the information contained in Refs. [3,5], and a recent remeasurement of the ^{28}Si(p,t)^{26}Si reaction [6]. Starting from the proton thresh-

TABLE II. Two possible scenarios for the states $E_x = 5-6$ MeV region seen in the ^{29}Si(^{3}He,^{6}He)^{26}Si reaction and comparison to expected Coulomb shifts from mirror states in ^{26}Mg as calculated in Ref. [5]. Scenario 2 is a much better fit.

	Scenario 1		Scenario 2	
Ex [MeV]	J^π	Δ [keV]	J^π	Δ [keV]
5.140	2^+	−65	2^+	−65
5.526	4^+	−88	4^+	−88
5.678	3^+	−292	1^+	40
5.945	1^+	307	3^+	−25

old, the state we see at $E_x = 5.526$ MeV was seen by Bardayan *et al.* at 5.515(2) MeV. Using angular distribution measurements, they determine this state has $J^\pi = 4^+$. This new information is consistent with the Coulomb shift calculated in Ref. [5], and repositions the fourth 4^+ state (located at 5.940 in Ref. [5]) to this location. In addition, Bardayan *et al.* also see a state at $E_x = 5.916(2)$ MeV, and their angular distribution is well fit by a $l = 0$ transfer; they assign this state as the fourth $J^\pi = 0^+$ state. This excitation energy measurement agrees well with the (^{3}He,n) data presented in Ref. [3], in which a state at $E_x = 5.91$ MeV is measured. This scenario now leaves only the 1^+ and the 3^+, the two unnatural parity states in the region of $E_x = 5-6$ MeV, unassigned.

The only remaining unexplained fact in the existing data is that the (^{3}He,n) angular distributions for the 5.91 MeV state in Ref. [3] could only be fit with a combination of 0^+ and 4^+ states. The 0^+ state should be populated strongly through direct transfer of a pair of protons, and consequently the angular distribution should show very clear $l = 0$ character. If the other member of the doublet is an unnatural parity state, it should be populated weakly with the ^{24}Mg(^{3}He,n)^{26}Si reaction, and it probably would not exhibit a distinctive angular distribution because the reaction mechanism is more complicated than direct transfer. Thus, the state would only appear in the minima of the 0^+ angular distribution, and would have a fairly featureless angular distribution. This, in fact, is in agreement with the (^{3}He,n) data in Ref. [3]. In addition, the Bohne *et al.* data show a small, high energy tail on the 5.91 MeV peak, also supporting this hypothesis. Thus we conclude the state we see at $E_x = 5.945$ MeV has unnatural parity.

Given these arguments, we now consider two possible scenarios, in which our states at $E_x = 5.678$ and 5.945 MeV are these two missing unnatural parity states, which are outlined in Table II. In the first scenario, we make the assignments $J^\pi = 3^+$ to the 5.678 MeV state and the $J^\pi = 1^+$ to the 5.945 MeV state. In the second scenario, we switch the J^π assignments. Using these assignments, we compared the excitation energies to calculated Coulomb-shifted levels from Ref. [5]. As can be seen from the table, the second scenario is a better fit to the expected location of these levels. A summary of suggested excitation energies and J^π for states up through 6 MeV in ^{26}Si is listed in Table I.

Using this second scenario, we have computed new reaction rates based on these new assignments (see Ref. [5] for formulas used) and present these rates in Fig. 5. The 4^+ state, having an $E_r = 8$ keV, does not contribute to the reaction rate. We used $E_x = 5.916$ MeV for the 0^+ state, taken from Ref. [6]. Proton widths were calculated based on the prescription in Ref. [11] for the old and new locations and assignments, to determine the behavior of the widths as a function of resonance energy. A ratio of these two calculations was computed, then applied to the values established in Ref. [5]. For the γ widths we used the experimental values based on ^{26}Mg mirror states [5], except for the 1^+ state, where we used the value calculated in Ref. [5] because the experimental value is only a lower limit. The corresponding resonance strengths used for the calculation were $\omega\gamma(0^+) = 3.6\times10^{-4}$ eV, $\omega\gamma(1^+) = 1.4\times10^{-9}$ eV, and $\omega\gamma(3^+) = 1.8\times10^{-2}$ eV. The direct capture rates were taken directly from Ref. [5]. As can be seen in the figure, the reaction rates are dominated by the two unnatural parity states in ^{26}Si in the temperature range of $T_9 = 0.05-1$.

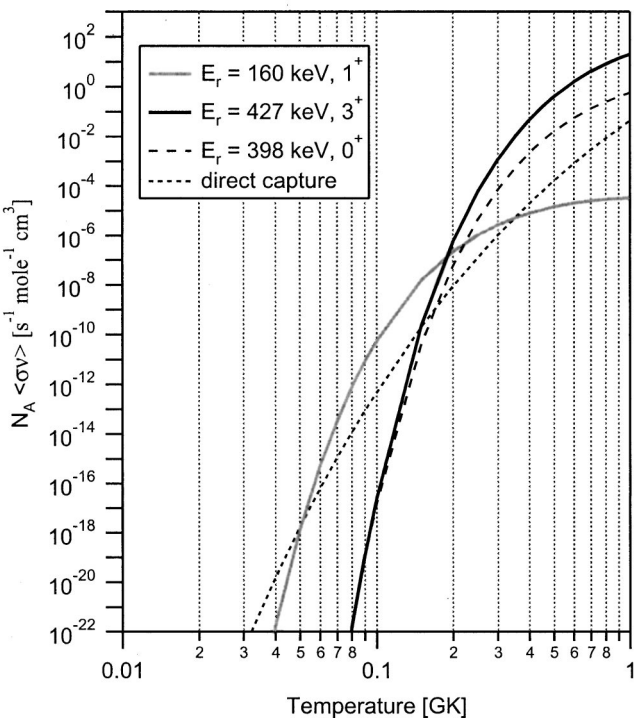

FIG. 5. A possible set of astrophysical reaction rates of the ^{25}Al(p,γ) reaction. Presented in this figure is the case where the $E_x = 5.678$ MeV state is the 1^+ state (thick gray line) and the $E_x = 5.945$ MeV state is the 3^+ state (thick black line). The 0^+ excitation energy is taken from Ref. [6], and the direct capture rates are taken directly from Ref. [5].

In order to truly assign astrophysical significance to these states, it is important to deduce their spins and parities and to measure their resonance strengths. This is difficult with the ^{29}Si(^{3}He,^{6}He)^{26}Si reaction, but can be done with a radioactive beam of ^{25}Al. Sufficiently intense beams of ^{25}Al should be available within a few years at several places. A measurement of elastic scattering in inverse kinematics should identify all of the important states within 1 MeV above the proton threshold. This ^{29}Si(^{3}He,^{6}He)^{26}Si measurement provides

a first indication about the energy regions that might be critical in those studies.

IV. CONCLUSIONS

We have studied the ^{29}Si(^{3}He,^{6}He)^{26}Si reaction at 51 MeV at an angle of 7.5°. We have identified new states in ^{26}Si at 5.140(10), 5.678(8), and 5.945(8) MeV. The 5.140 MeV state is consistent with a state at 5.145(2) reported in a recent remeasurement of the ^{28}Si$(p,t)^{26}$Si reaction at ORNL [6], but that experiment did not see states at 5.678 or 5.945 MeV, strengthening the hypothesis that the states seen in this measurement of the ^{29}Si(^{3}He,^{6}He)^{26}Si reaction are unnatural parity states. Reaction rates have been presented based on the most likely scenario, in light of recent evidence, that the 5.678 MeV state is the missing $J^{\pi}=1^{+}$ state and that the 5.945 MeV state is the $J^{\pi}=3^{+}$ state. Unfortunately, it is difficult to determine the spin-parity of the two new states from the angular distributions, as this reaction is not well suited for that purpose. Though it has been done in the past (see Ref. [12], for example), it does not uniquely determine the spin parity of the level. However, future experiments with beams of ^{25}Al can be used to measure the properties of the states above the proton threshold which are important for the production of ^{26}Al^{0} in novae.

ACKNOWLEDGMENTS

This work was supported by the U.S. Department of Energy, Grant Nos. W-31-109-ENG-38 and DE-FG02-91ER-40609.

[1] R. Diehl *et al.*, Astron. Astrophys. **97**, 181 (1993).
[2] R.A. Paddock, Phys. Rev. C **5**, 485 (1972).
[3] W. Bohne, K.D. Buchs, H. Fuchs, K. Grabisch, D. Hilscher, U. Jahnke, H. Kluge, T.G. Masterson, H. Morgenstern, and B.W. Wildenthal, Nucl. Phys. **A378**, 525 (1982).
[4] W.P. Alford, P. Craig, D.A. Lind, R.S. Raymond, J. Ullman, C.D. Zafiratos, and B.H. Wildenthal, Nucl. Phys. **A457**, 317 (1986).
[5] C. Iliadis, L. Buchmann, P.M. Endt, H. Herndl, and M. Wiescher, Phys. Rev. C **53**, 475 (1996).
[6] D. Bardayan *et al.*, Phys. Rev. C **65**, 032801(R) (2002).
[7] A. Chen, Ph.D. thesis, 1999 (unpublished).
[8] G. Audi and A.H. Wapstra, Nucl. Phys. **A595**, 409 (1995).
[9] P.M. Endt, Nucl. Phys. **A521**, 1 (1990).
[10] P.M. Endt, Nucl. Phys. **A633**, 1 (1998).
[11] C. E. Rolfs and W. S. Rodney, *Cauldrons in the Cosmos* (The University of Chicago Press, Chicago, 1988).
[12] V. Guimaraes *et al.*, Phys. Rev. C **58**, 116 (1998).